NATIONAL CENTER FOR EARTHQUAKE
ENGINEERING RESEARCH
State University of New York at Buffalo

HORIZONTAL IMPEDANCES FOR RADIALLY INHOMOGENEOUS VISCOELASTIC SOIL LAYERS

by

A. S. Veletsos and K. W. Dotson
Department of Civil Engineering
Rice University
Houston, TX 77251

Technical Report NCEER-87-0021

October 15, 1987

This research was conducted at Rice University and was partially supported by the National Science Foundation under Grant No. ECE 86-07591

NOTICE

This report was prepared by Rice University as a result of research sponsored by the National Center for Earthquake Engineering Research (NCEER). Neither NCEER, associates of NCEER, its sponsors, Rice University, nor any person acting on their behalf:

a. makes any warranty, express or implied, with respect to the use of any information, apparatus, method, or process disclosed in this report or that such use may not infringe upon privately owned rights; or

b. assumes any liabilities of whatsoever kind with respect to the use of, or for damages resulting from the use of, any information, apparatus, method or process disclosed in this report.

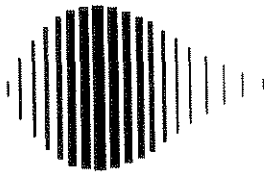

HORIZONTAL IMPEDANCES FOR RADIALLY INHOMOGENEOUS VISCOELASTIC SOIL LAYERS

by

A.S. Veletsos[1] and K.W. Dotson[2]

October 15, 1987

Technical Report NCEER-87-0021

NCEER Contract Number 86-2034

NSF Master Contract Number ECE 86-07591

1 Brown and Root Professor, Dept. of Civil Engineering, Rice University
2 Graduate Student, Dept. of Civil Engineering, Rice University

NATIONAL CENTER FOR EARTHQUAKE ENGINEERING RESEARCH
State University of New York at Buffalo
Red Jacket Quadrangle, Buffalo, NY 14261

ACKNOWLEDGMENT

This study was supported in part by an ARCS Foundation Scholarship awarded through Rice University to K. W. Dotson, and in part by Grant 86-2034 from the National Center for Earthquake Engineering Research, State University of New York at Buffalo. This support is appreciated greatly. The study also benefited from a lecture on the same general topic presented at Rice University by Professor J. M. Roesset of the University of Texas at Austin.

ABSTRACT

A study of the dynamic impedances of horizontally excited, radially inhomogeneous, infinite viscoelastic soil layers with a circular hole, and of piles embedded in a medium represented by such layers is made considering the shear modulus of the material to increase radially within a narrow annular boundary zone. Unlike a previous study in which the boundary zone was presumed to be massless, in the present study the inertia effects of this zone are taken into account. The impedances are evaluated over wide ranges of the parameters involved and the sensitivity of the results is assessed. The results are also compared with those obtained for similarly excited homogeneous layers and for vertically excited inhomogeneous layers. For purposes of analysis, the inhomogeneous boundary zone is represented by a series of concentric rings of constant properties, and the transfer matrix technique is used to evaluate the results. The analysis and the computer program used to implement it are applicable to layers of arbitrary radial variation of material properties.

TABLE OF CONTENTS

LIST OF ILLUSTRATIONS

LIST OF TABLES

SECTION 1
INTRODUCTION

One of the more efficient and reliable approximate methods for evaluating the dynamic response of piles and other embedded foundations is the one proposed by Novak and his associates [4,5,6], in which the restraining action of the surrounding soil is expressed in the spirit of the Winkler approach by a series of independent springs and dashpots arranged in parallel. The dynamic properties of these elements are computed considering the soil to act as a series of thin independent layers of infinite extent in the horizontal plane. This approach effectively assumes that waves in the soil propagate only horizontally by shearing and extensional actions.

The early evaluations of the dynamic layer impedances were based on Baranov's solution [4] which is applicable to homogeneous layers. The assumption of radial homogeneity is generally not realistic, however, because construction operations disturb the soils in the immediate vicinity of a foundation and reduce their shear moduli.

To provide for the reduced resistance of the soil around the foundation, Novak and Sheta [7] have proposed the use of a composite layer for which the shear modulus within a narrow annular boundary zone is lower than for the rest of the medium, and have evaluated the relevant impedances considering the boundary zone to be massless. Subsequent analyses by the writers for vertically and torsionally excited layers [10] revealed that the inertia effects of the boundary zone may be quite substantial and should not, in general, be neglected.

A comprehensive study of the impedances of composite layers in vertical and torsional modes of vibration has been reported in Reference [11] using the rigorous method of analysis. As a sequel to this contribution, the present paper presents the results of a corresponding study for horizontally excited layers.

The dynamic impedances of such layers are evaluated over wide ranges of the parameters involved, and the results are compared with those obtained for similarly excited homogeneous layers and for vertically excited composite layers. The shear modulus of the soil within the boundary zone is assumed

to increase linearly in the radial direction in these solutions. This assumption is considered to be more realistic than that of constant modulus employed previously. In addition, several other variations of material properties are examined, and the sensitivity of the results to the various factors involved is assessed. A secondary objective of the paper is to assess the effects that the horizontal inhomogeneity in soil properties has on the dynamic impedances of representative piles excited horizontally or rotationally.

In the method of analysis employed, the radially inhomogeneous boundary zone is replaced by a series of concentric rings of constant properties, and the transfer matrix technique is used to evaluate the desired impedances. The method of analysis and the computer program used to implement it are applicable to layers with arbitrary radial variations of material properties. The analysis is highly efficient and the reported data are believed to be of high accuracy.

The response of horizontally excited composite layers was also examined by Lakshmanan and Minai in [3], but the shear modulus of the material within the boundary zone was effectively considered to be constant in this study.

SECTION 2
SYSTEM EXAMINED

The system investigated is similar to that considered in the study of vertically and torsionally excited layers presented in Reference 11. It is a thin viscoelastic soil layer of unit depth and infinite extent with a circular hole of radius R, as shown in Figure 2-1(a). The layer consists of two concentric zones: a narrow annular inner zone of disturbed or softened material, and a semi-infinite outer zone of undisturbed material. Unlike the previously examined system, however, for which the material properties within each zone were considered to be constant, in the present system those for the inner zone are presumed to be constant in the circumferential direction and to vary arbitrarily in the radial direction. As before, the properties of the outer zone are taken as constant.

The layer is excited horizontally by a harmonic force which is distributed along the boundary of the hole so as to displace that boundary as a rigid body without distortion. It is desired to evaluate the dynamic impedance of the layer, K_u, defined as the complex-valued amplitude of the total horizontal force which is necessary to produce a steady-state horizontal displacement of unit amplitude in the direction of the excitation.

The width of the annular zone and the radius of the boundary of the two zones are denoted by ΔR and R_o, respectively. The location of an arbitrary point is defined by the polar coordinates, ξ and θ, in which $\xi = r/R$, r = the radial distance to the point under consideration, and θ is measured counterclockwise from an axis parallel to the direction of the applied force. The soil properties for an arbitrary point are defined by its mass density, ρ, Poisson's ratio, ν, and the complex-valued quantities

$$G^* = G(1 + i\tan\delta_s) \tag{1a}$$

and

$$\Lambda^* + 2G^* = (\Lambda + 2G)(1 + i\tan\delta_\ell) \tag{1b}$$

in which G = the shear modulus of elasticity, Λ = the second Lame constant, and $\tan\delta_s$ and $\tan\delta_\ell$ are the material damping values for shearing and longitudinal distortion, respectively. The latter quantities are presumed to

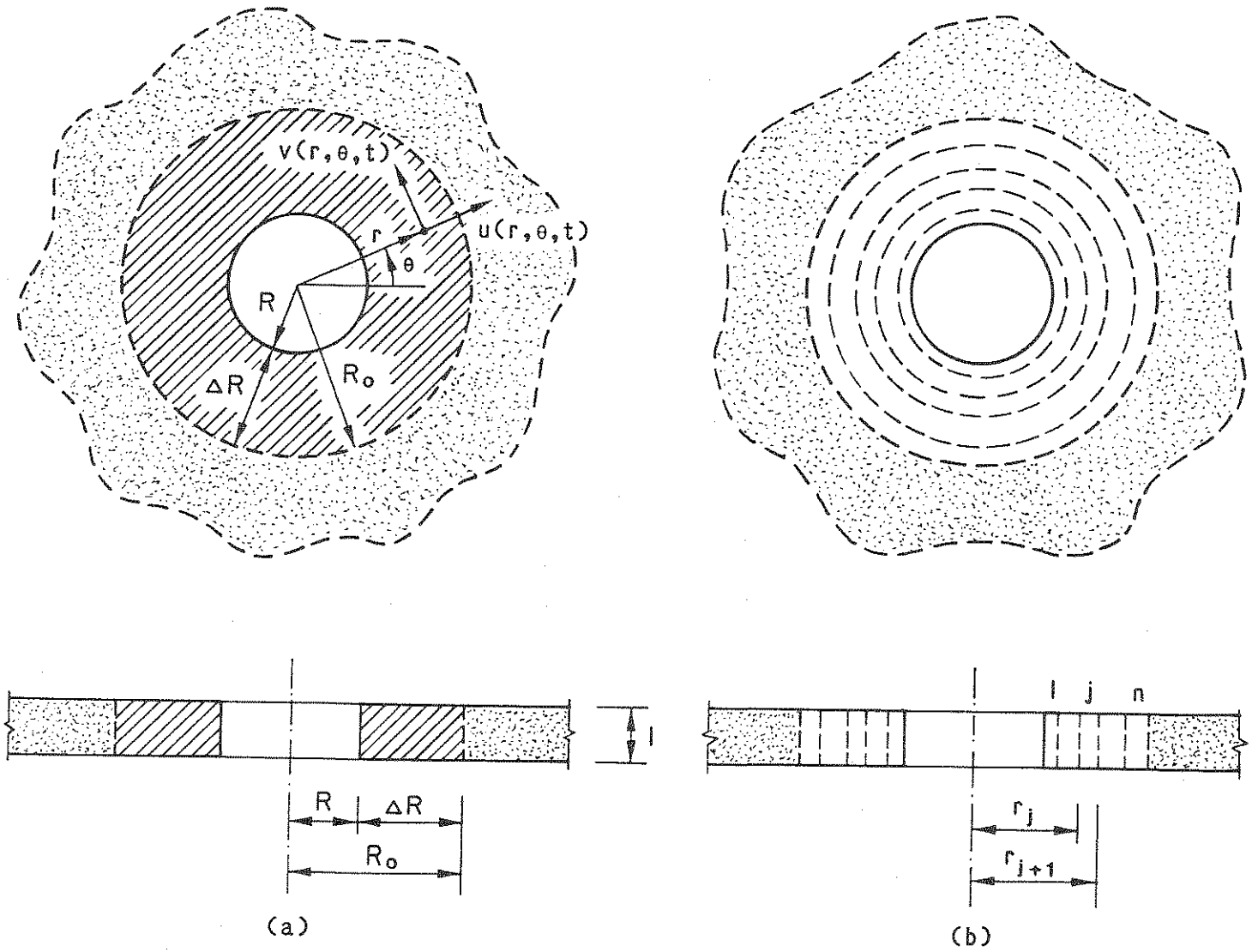

FIGURE 2-1 System Considered and Discretization of Boundary Zone

be independent of the frequency of the excitation. The material properties along the boundary of the circular hole are identified with the subscript 'i', and those of the outer region are identified with the subscript 'o'. While the material damping values for shearing and longitudinal actions are considered to be different in the formulation of the analysis, in the numerical solutions, they are presumed to be the same and are denoted by $\tan\delta$.

SECTION 3
METHOD OF ANALYSIS

Inasmuch as an exact solution of the governing equations of motion for an arbitrary radial variation of material properties is not possible, the inner zone of the layer is approximated by a series of concentric rings of constant properties, as shown in Figure 2-1(b). The analysis of the system is then implemented by repeated application of the solution for a layer of constant properties.

The substitute rings are numbered from 1 to n, starting with the one adjoining the hole and terminating with the one adjoining the undisturbed outer soil region. The radii of the inner and outer boundaries of the jth ring are denoted by r_j and r_{j+1}, and the radii r_1 and r_{n+1} are also denoted by R and R_o, respectively. In an analogous manner, the subscripts 1 and i are used interchangeably to identify the properties of the innermost ring; and the subscripts n + 1 and o are used interchangeably to identify the properties of the undisturbed outer zone.

3.1 Fundamental Relations

Let $u = u(r,\theta,t)$ and $v = v(r,\theta,t)$ be, respectively, the radial and circumferential components of the displacement at time t of a point on an arbitrary ring. On the assumption that the layer deforms horizontally with no vertical distortion, u and v may be expressed in terms of the potential functions ϕ and ψ in a form analogous to that employed in Reference 6, as:

$$u = \frac{\partial \phi}{\partial \xi} + \frac{1}{\xi}\frac{\partial \psi}{\partial \theta} \tag{2a}$$

$$v = \frac{1}{\xi}\frac{\partial \phi}{\partial \theta} - \frac{\partial \psi}{\partial \xi} \tag{2b}$$

By appropriate readjustment of the relevant expressions presented in the latter reference, it can then be shown that the motion is governed by the following system of uncoupled differential equations

$$\frac{v_\ell^2(1+i\tan\delta_\ell)}{R^2}\left(\frac{\partial^2\phi}{\partial\xi^2} + \frac{1}{\xi}\frac{\partial\phi}{\partial\xi} + \frac{1}{\xi^2}\frac{\partial^2\phi}{\partial\theta^2}\right) = \frac{\partial^2\phi}{\partial t^2} \tag{3a}$$

$$\frac{v_s^2(1+i\tan\delta_s)}{R^2}\left(\frac{\partial^2\psi}{\partial\xi^2}+\frac{1}{\xi}\frac{\partial\psi}{\partial\xi}+\frac{1}{\xi^2}\frac{\partial^2\psi}{\partial\theta^2}\right)=\frac{\partial^2\psi}{\partial t^2} \tag{3b}$$

in which $v_s = \sqrt{G/\rho}$ = the shear wave velocity for the material of the ring under consideration, $v_\ell = \varepsilon v_s$ = the corresponding longitudinal wave velocity, and

$$\varepsilon = \sqrt{\frac{\Lambda + 2G}{G}} = \sqrt{\frac{2(1-\nu)}{1-2\nu}} \tag{4}$$

The normal radial stress, $\sigma_r = \sigma_r(r,\theta,t)$, and the corresponding shearing stress, $\tau_{r\theta} = \tau_{r\theta}(r,\theta,t)$, may then be computed from (e.g., Reference 1)

$$\sigma_r = \frac{\Lambda^* + 2G^*}{R}\left(\frac{\partial u}{\partial\xi}+\frac{u}{\xi}+\frac{1}{\xi}\frac{\partial v}{\partial\theta}\right) - 2\frac{G^*}{R}\left(\frac{u}{\xi}+\frac{1}{\xi}\frac{\partial v}{\partial\theta}\right) \tag{5a}$$

and

$$\tau_{r\theta} = \frac{G^*}{R}\left(\frac{\partial v}{\partial\xi}-\frac{v}{\xi}+\frac{1}{\xi}\frac{\partial u}{\partial\theta}\right) \tag{5b}$$

For a harmonic mode of vibration, the potential functions and the displacement and stress components are of the form

$$\phi = \Phi(\xi)\cos\theta\, e^{i\omega t} \tag{6a}$$

$$\psi = \Psi(\xi)\sin\theta\, e^{i\omega t} \tag{6b}$$

$$u = U(\xi)\cos\theta\, e^{i\omega t} \tag{7a}$$

$$v = V(\xi)\sin\theta\, e^{i\omega t} \tag{7b}$$

$$\sigma_r = \sigma(\xi)\cos\theta\, e^{i\omega t} \tag{8a}$$

$$\tau_{r\theta} = \tau(\xi)\sin\theta\, e^{i\omega t} \tag{8b}$$

Equations (3) in this case reduce to ordinary differential equations, the solutions of which are

$$\Phi(\xi) = A K_1(\mu\xi) + B I_1(\mu\xi) \tag{9a}$$

$$\Psi(\xi) = C K_1(\lambda\xi) + D I_1(\lambda\xi) \tag{9b}$$

where

$$\lambda = \frac{i\omega R}{v_s\sqrt{1 + i\tan\delta_s}} \tag{10a}$$

$$\mu = \frac{i\omega R}{v_\ell\sqrt{1 + i\tan\delta_\ell}} = \frac{1}{\varepsilon}\frac{i\omega R}{v_s\sqrt{1 + i\tan\delta_\ell}} \tag{10b}$$

I_1 and K_1 are modified Bessel functions of the first order of the first and second kind, respectively, and A through D are constants of integration that must be determined from the boundary conditions of the ring under consideration.

On substituting equations (6) and (7) along with equations (9) into equations (2), one obtains the following expressions for the displacement amplitudes:

$$U_j(\xi) = - A_j[\mu_j K_o(\mu_j\xi) + \frac{1}{\xi}K_1(\mu_j\xi)] + B_j[\mu_j I_o(\mu_j\xi) - \frac{1}{\xi}I_1(\mu_j\xi)]$$
$$+ C_j\frac{1}{\xi}K_1(\lambda_j\xi) + D_j\frac{1}{\xi}I_1(\lambda_j\xi) \tag{11a}$$

and

$$V_j(\xi) = - A_j\frac{1}{\xi}K_1(\mu_j\xi) - B_j\frac{1}{\xi}I_1(\mu_j\xi) + C_j[\lambda_j K_o(\lambda_j\xi) + \frac{1}{\xi}K_1(\lambda_j\xi)]$$
$$- D_j[\lambda_j I_o(\lambda_j\xi) - \frac{1}{\xi}I_1(\lambda_j\xi)] \tag{11b}$$

in which the subscripts on I and K denote the order of the Bessel functions involved and the subscripts j have been added to emphasize the fact that these expressions refer to the jth ring. The following expressions for the stress amplitudes are similarly obtained from equations (5) by making use of equations (7) and (8):

$$\sigma_j(\xi) = \frac{G_j^*}{R}\left\{A_j[\lambda_j^2 K_1(\mu_j\xi) + \frac{2\mu_j}{\xi}K_2(\mu_j\xi)] + B_j[\lambda_j^2 I_1(\mu_j\xi) - \frac{2\mu_j}{\xi}I_2(\mu_j\xi)]\right.$$

$$\left. - C_j\frac{2\lambda_j}{\xi}K_2(\lambda_j\xi) + D_j\frac{2\lambda_j}{\xi}I_2(\lambda_j\xi)\right\} \qquad (12a)$$

and

$$\tau_j(\xi) = \frac{G_j^*}{R}\left\{A_j\frac{2\mu_j}{\xi}K_2(\mu_j\xi) - B_j\frac{2\mu_j}{\xi}I_2(\mu_j\xi)\right.$$

$$\left. - C_j[\lambda_j^2 K_1(\lambda_j\xi) + \frac{2\lambda_j}{\xi}K_2(\lambda_j\xi)] - D_j[\lambda_j^2 I_1(\lambda_j\xi) - \frac{2\lambda_j}{\xi}I_2(\lambda_j\xi)]\right\} \qquad (12b)$$

Equations (11) and (12) can also be applied to the semi-infinite outer zone of constant material properties ($\xi > 1 + \Delta R/R$) provided the subscript j is interpreted as $n + 1 = o$, and the integration constants B_j and D_j are taken as zero so as to satisfy the condition of vanishing displacements as $\xi \to \infty$.

3.2 Solution of Equations

Let $\{X_j\} = \{A_j\ B_j\ C_j\ D_j\}^T$ be the vector of the constants of integration in equations (11) and (12), and $\{S_j(\xi)\} = \{U_j(\xi)\ V_j(\xi)\ \sigma_j(\xi)\ \tau_j(\xi)\}^T$ be the vector of the corresponding displacement and stress amplitudes. For $j = n + 1 = o$, the vectors $\{X_j\}$ and $\{S_j(\xi)\}$ specialize to $\{X_o\} = \{A_o\ C_o\}^T$ and $\{S_o(\xi)\} = \{U_o(\xi)\ V_o(\xi)\ \sigma_o(\xi)\ \tau_o(\xi)\}^T$. The relationship between $\{X_j\}$ and $\{S_j(\xi)\}$ may then be expressed as

$$\{S_j(\xi)\} = [d_j(\xi)]\{X_j\} \qquad \text{for } 1 \le j \le n \qquad (13a)$$

$$\{S_o(\xi)\} = [d_o(\xi)]\{X_o\} \qquad \text{for } j = n + 1 = o \qquad (13b)$$

in which $[d_j(\xi)]$ and $[d_o(\xi)]$ are matrices of size 4 x 4 and 4 x 2, respectively, whose elements are determined from equations (11) and (12).

The conditions that must be satisfied are that the displacements and stresses are continuous at the ring interfaces, and that the boundary of the circular hole experiences a rigid body motion of unit amplitude. The

first condition requires that

$$\{S_j(\xi_{j+1})\} = \{S_{j+1}(\xi_{j+1})\} \tag{14}$$

in which $\xi_{j+1} = r_{j+1}/R$ = the value of ξ corresponding to the interface of the j and j+1 rings, whereas the second condition requires that

$$\begin{Bmatrix} U_1(1) \\ V_1(1) \end{Bmatrix} = [\tilde{d}_1(1)]\{X_1\} = \begin{Bmatrix} 1 \\ -1 \end{Bmatrix} \tag{15}$$

in which $[\tilde{d}_1(1)]$ is a 2 x 4 matrix whose elements are identical to those of the first two rows of $[d_1(1)]$. The horizontal impedance of the layer, K_u, is then given by:

$$K_u = -\int_0^{2\pi} [\sigma_1(1)\cos^2\theta - \tau_1(1)\sin^2\theta]\, R\, d\theta$$

$$= \pi G_i a_i^2 [K_1(\mu_1)\ \ I_1(\mu_1)\ \ K_1(\lambda_1)\ \ I_1(\lambda_1)]\{X_1\} \tag{16}$$

in which a_i is a dimensionless frequency parameter defined by

$$a_i = \frac{\omega R}{v_{si}} \tag{17}$$

and $v_{si} = \sqrt{G_i/\rho_i}$ = the shear wave velocity for a medium having the properties of the layer along the boundary of the hole.

The vector $\{X_1\}$ in equation (16) may conveniently be determined by application of the transfer matrix technique as follows. Substitution of equation (13a) into equation (14) yields the following relation between $\{X_j\}$ and $\{X_{j+1}\}$

$$\{X_j\} = [d_j(\xi_{j+1})]^{-1}[d_{j+1}(\xi_{j+1})]\{X_{j+1}\} \tag{18a}$$

which, for j = n, specializes to

$$\{X_n\} = [d_n(\xi_o)]^{-1}[d_o(\xi_o)]\{X_o\} \tag{18b}$$

with $\xi_o = R_o/R = 1 + \Delta R/R$. By successive application of these expressions to the interfaces defined by ξ_2 through $\xi_{n+1} = \xi_o$, the vector $\{X_1\}$ for the innermost ring may be related to the vector $\{X_o\}$ for the semi-infinite outer zone by:

$$\{X_1\} = [T]\{X_o\} \tag{19}$$

in which [T] is a 4 x 2 transfer matrix defined by

$$[T] = [d_1(\xi_2)]^{-1}[d_2(\xi_2)][d_2(\xi_3)]^{-1}[d_3(\xi_3)]\ldots[d_n(\xi_o)]^{-1}[d_o(\xi_o)]$$

$$= \prod_{j=1}^{j=n} [d_j(\xi_{j+1})]^{-1}[d_{j+1}(\xi_{j+1})] \tag{20}$$

On substituting equation (19) into equation (15) and taking the inverse, one obtains

$$\{X_o\} = \left([\tilde{d}_1(1)][T]\right)^{-1} \begin{Bmatrix} 1 \\ -1 \end{Bmatrix} \tag{21}$$

With $\{X_o\}$ determined, the vector $\{X_1\}$ is evaluated from equation (19), and the desired impedance of the layer is computed from equation (16).

SECTION 4
PRESENTATION AND ANALYSIS OF RESULTS

4.1 Form of Presentation

Equation (16) may conveniently be expressed in the form

$$K_u = 1.5\pi G_i(\alpha_u + ia_i\beta_u) \tag{22}$$

in which α_u and β_u are dimensionless factors that depend on a_i, $\Delta R/R$, G_o/G_i, ρ_o/ρ_i, ν_i, ν_o, $\tan\delta_i$, $\tan\delta_o$, and the forms of radial variation of material properties within the narrow boundary zone. For the data presented herein, both ρ and ν are considered to be constant throughout, and ν is taken as 1/3.

The real part of equation (22) represents the force component that is in phase with the motion, and the imaginary part represents the component that is 90° out of phase. In an equivalent, spring-dashpot representation of the soil layer, the spring stiffness is represented by the real part of equation (22), and the damping coefficient, c_u, is related to β_u by the expression

$$c_u = 1.5\pi\beta_u \frac{G_i R}{v_{si}} \tag{23}$$

The quantities α_u and β_u will be referred to as the impedance coefficients.

In conformity with the format used for the corresponding expression in Reference 11, equation (22) is expressed in terms of the shear modulus of the layer along the boundary of the central hole rather than that of the outer zone, and the factor a_i has been inserted in front of β_u. When expressed in this manner, the high-frequency limit of α_u for a homogeneous layer with $\nu = 1/3$ and no material damping is unity, and the corresponding limit of $\beta_u = 2$. For a homogeneous layer with an arbitrary value of ν, these high-frequency limits are given by

$$\alpha_u\Big|_{a_o\to\infty} = \frac{2}{3}\varepsilon - \frac{1}{3}(\varepsilon - 1)^2 \tag{24a}$$

$$\beta_u\Big|_{a_o\to\infty} = \frac{2}{3}(\varepsilon + 1) \tag{24b}$$

These expressions are obtained from the relevant expression for the dynamic impedance presented in References [5] and [6] by replacing the Bessel functions involved with their asymptotic expansions for large arguments.

The variations of α_u and β_u for a homogeneous viscoelastic layer with $\nu = 1/3$ and three different values of $\tan\delta$ are shown in Figure 4-1 as a function of the frequency parameter $a_i = a_o = \omega R/v_s$, in which v_s = the velocity of shear wave propagation in the layer.

4.2 Impedance Coefficients

The impedance coefficients α_u and β_u have been evaluated for a layer for which the shear modulus within the boundary zone increases linearly from G_i to G_o in the radial direction. The results are plotted in Figure 4-2 as a function of a_i for several different values of $\Delta R/R$ and G_o/G_i and two values of material damping. The solid curves refer to an elastic layer, whereas the dashed curves refer to a viscoelastic layer for which the material damping factors for both longitudinal and shearing deformations vary inversely with $G(\xi)$, as follows:

$$\tan\delta(\xi) = \begin{cases} \dfrac{G_o}{G(\xi)} \tan\delta_o & \text{for } 1 \leq \xi \leq \xi_o \\ \tan\delta_o & \text{for } \xi \geq \xi_o \end{cases} \qquad (25)$$

in which $\tan\delta(\xi)$ = the material damping factor at an arbitrary value of ξ, and $\tan\delta_o$ = the corresponding factor for the outer region. The variation represented by equation (25) is intended to approximate the known increase in the damping capacity of soils with increasing strain level and the associated reduction in the effective value of the shear modulus. For the solutions displayed in Figure 4-2, $\tan\delta_o = 0.05$. The corresponding value of $\tan\delta_i = \tan\delta(1)$ is 0.10 for $G_o/G_i = 2$, and 0.20 for $G_o/G_i = 4$.

The following trends may be observed from Figure 4-2:

1. Both α_u and β_u generally increase with increasing ratio of the shear moduli, G_o/G_i, the increase being larger for α_u than for β_u.

2. At low values of the frequency parameter, the increase in α_u is essen-

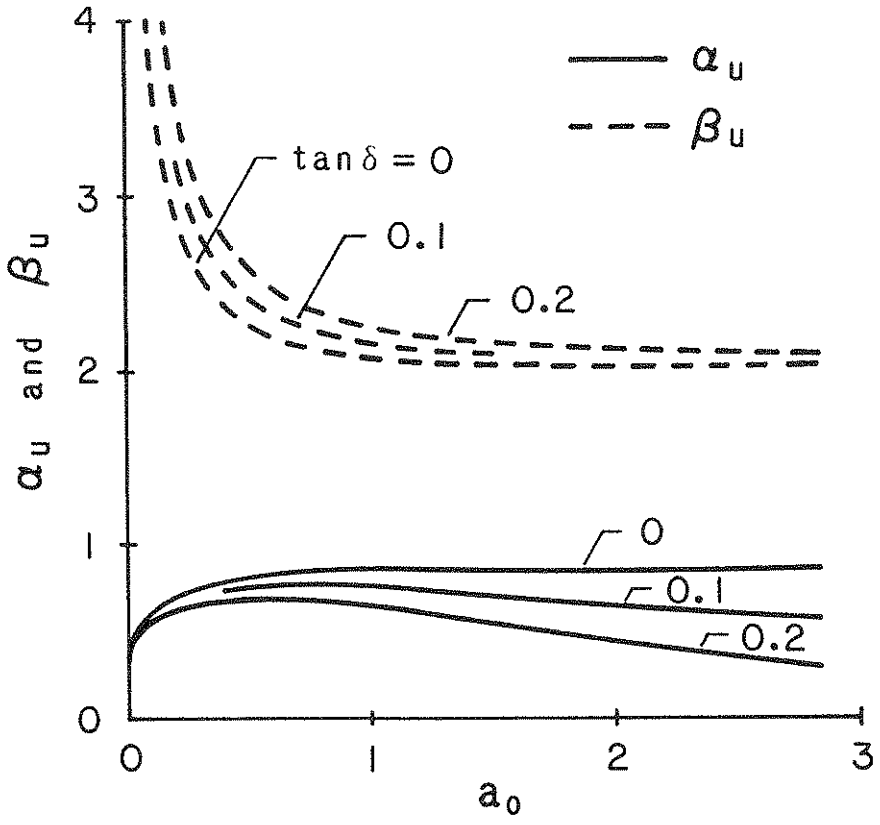

FIGURE 4-1 Impedance Coefficients for Homogeneous Viscoelastic Soil Layers with ν = 1/3

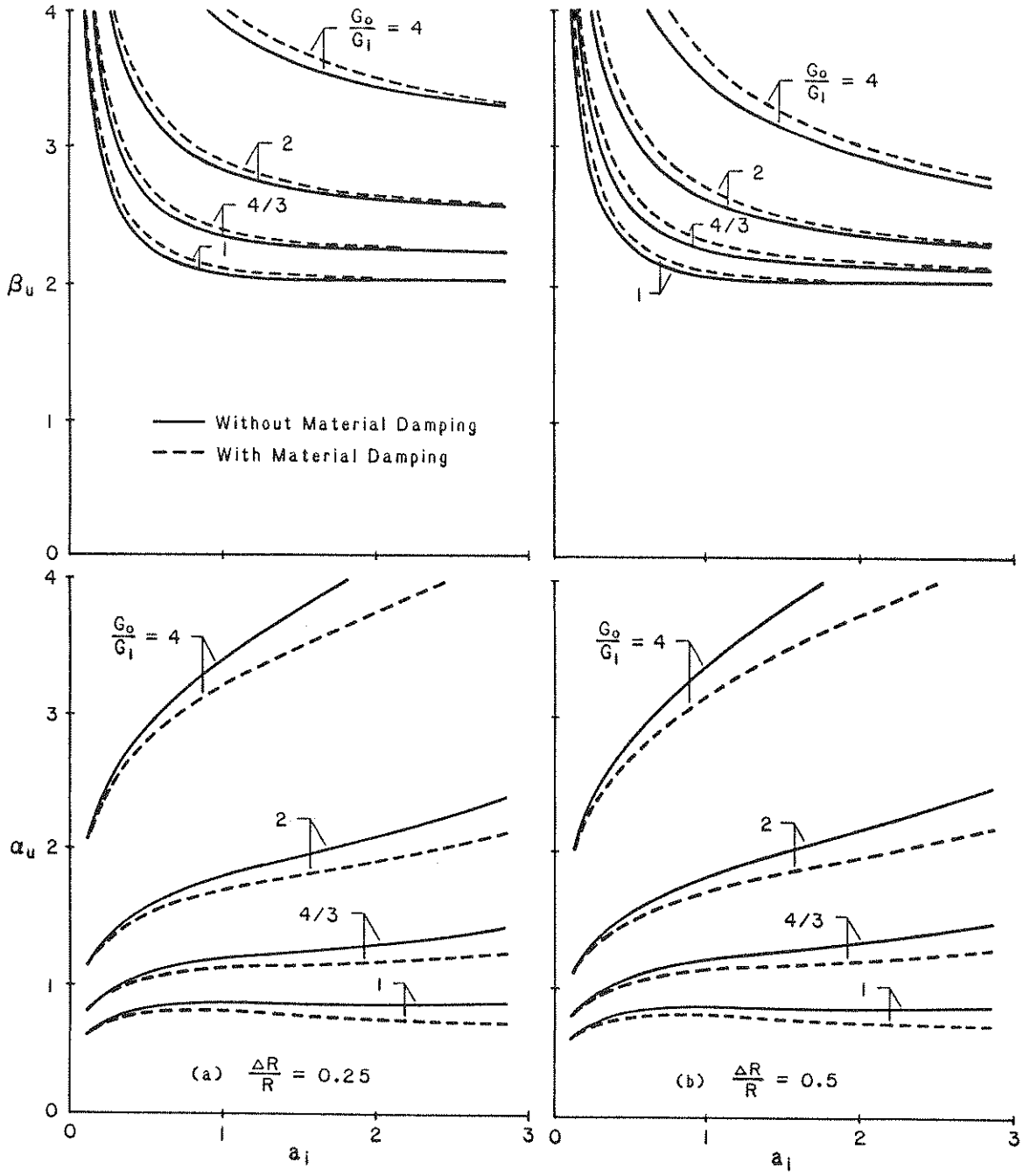

FIGURE 4-2 Impedance Coefficients for Soil Layers with Linearly Increasing Shear Modulus within Boundary Zone; ν = 1/3 (Figure continued)

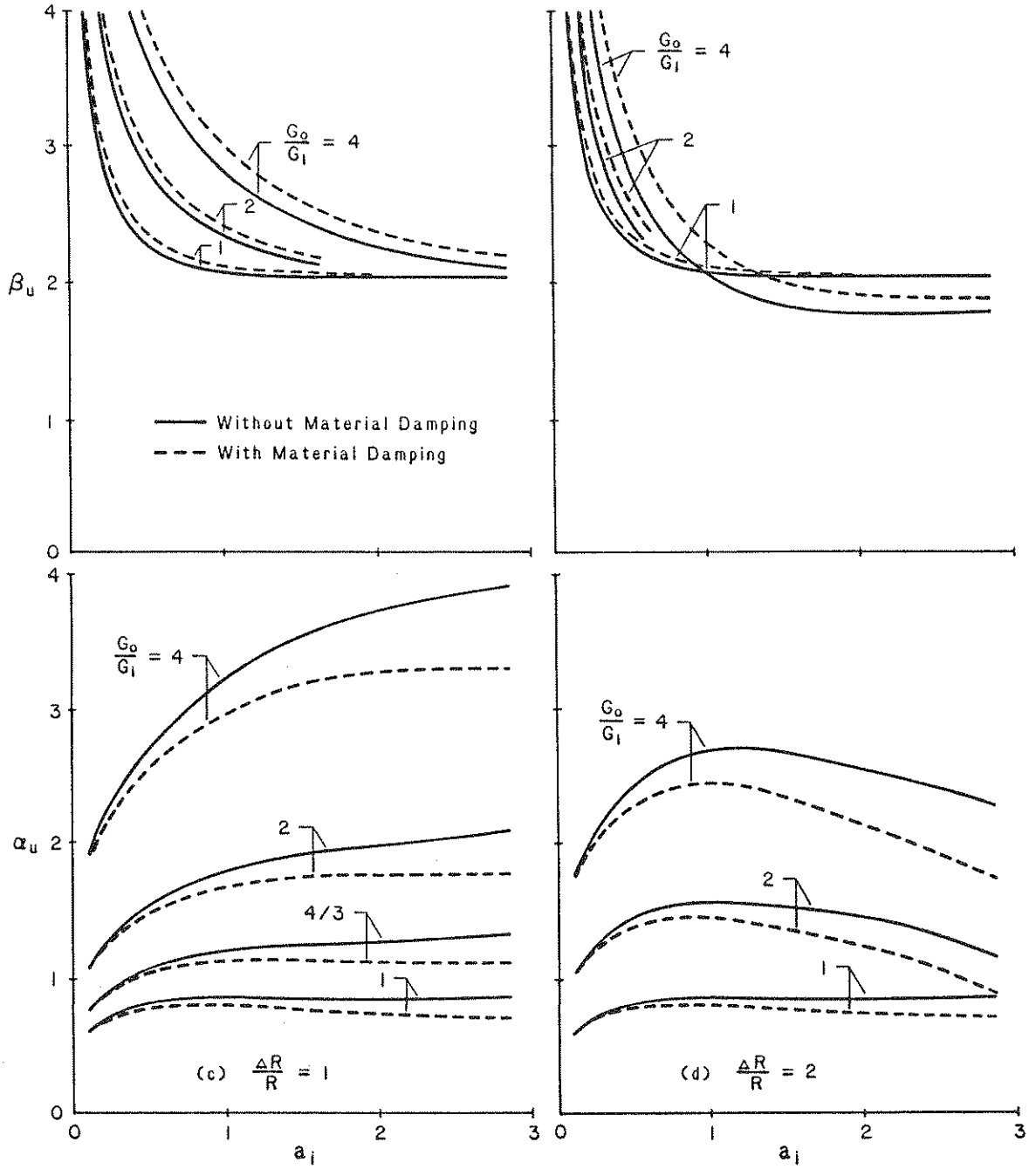

FIGURE 4-2 Concluded

tially proportional to G_o/G_i, whereas the increase in β_u is approximately proportional to $\sqrt{G_o/G_i}$. As explained in Reference [11] for vertically excited layers with constant material properties within each zone, these proportionalities follow from the fact that the response of the layer in this case is effectively controlled by the properties of the outer soil region.

3. The curves for the lower values of $\Delta R/R$ are essentially stretched-out versions of the initial portions of the curves for the higher values of $\Delta R/R$. As a result, the range of a_i values within which the aforementioned proportionalities may be considered to be valid increases with decreasing $\Delta R/R$. These trends are consequences of the fact that the response of a composite layer is controlled not so much by a_i as by the frequency ratio ω/p_1, in which p_1 = the fundamental circular natural frequency of horizontal vibration for the inner zone when its outer boundary is fixed. Since the latter frequency is essentially inversely proportional to ΔR, the smaller the ratio $\Delta R/R$, the larger is the value of a_i corresponding to a prescribed ω/p_1. This reasoning was also used to explain related trends in the results for the vertically excited layers presented in Reference [11], and it is pursued further in a later section.

4. Over the entire range of a_i values examined, which is substantially broader than that normally encountered in studies of pile foundations, the curves for both α_u and β_u are smooth and exhibit either no or only minor undulations. By contrast, the previously reported curves for the vertically excited layers [11] are dominated by undulations of substantial amplitudes, caused by the abrupt change in shear modulus at the boundary of the two zones and the associated wave reflections from that boundary.

5. As would be expected from available information (e.g., Reference 5), material damping decreases the values of α_u and increases the values of β_u.

4.3 Behavior at High Frequencies

Although values of layer impedances for $a_i > 3$ are needed infrequently in

practice, it is nevertheless desirable to examine their behavior for this frequency range. In Figure 4-3 are given representative plots of α_u and β_u for an elastic layer with values of a_i up to 8. Note that, for the higher values of a_i, the curves are undulatory; that the undulations are larger for the α_u-curves than the β_u-curves; and that the amplitudes of the undulations increase with increasing G_o/G_i and decreasing $\Delta R/R$.

A consequence of the discontinuity in the slope of $G(\xi)$ at the interface of the two zones, these undulations increase with increasing magnitude of the discontinuity but are of significantly smaller amplitude than those due to a discontinuity in $G(\xi)$ itself. This matter is examined further in a subsequent section.

In the study of vertically and torsionally excited layers reported in Reference [11], and in a related previous study by Gazetas and Dobry [2], it was shown that the high-frequency limit of the imaginary part of the impedance function depends solely on the value of the shear modulus at the boundary of the hole, G_i. In the words of Gazetas and Dobry, "the source" in this case "sees the transmitting medium as a homogeneous medium" with properties equal to those of the medium in the immediate vicinity of the hole. This statement is strictly valid only for layers for which both $G(\xi)$ and its first derivative, $G'(\xi)$, are continuous. For discontinuous variations, the curves for β_u tend to oscillate about the aforementioned high-frequency limit, but the amplitudes of the oscillations due to a discontinuity in $G'(\xi)$, as already indicated, are generally quite small and are further suppressed by material damping.

By contrast to the high-frequency limit of the imaginary part of the impedance function which effectively depends on G_i, the corresponding limit of the real part for the vertically and torsionally excited layers examined in Reference [11] was shown to depend, in addition, on the value of G_i', the first derivative of $G(\xi)$ at $\xi = 1$. That this is also true for laterally excited layers is demonstrated in Figure 4-4, in which curves for α_u are given for three elastic layers for which the detailed variations of $G(\xi)$ are different but their initial values and initial slopes are the same. Variation 'A' is defined by

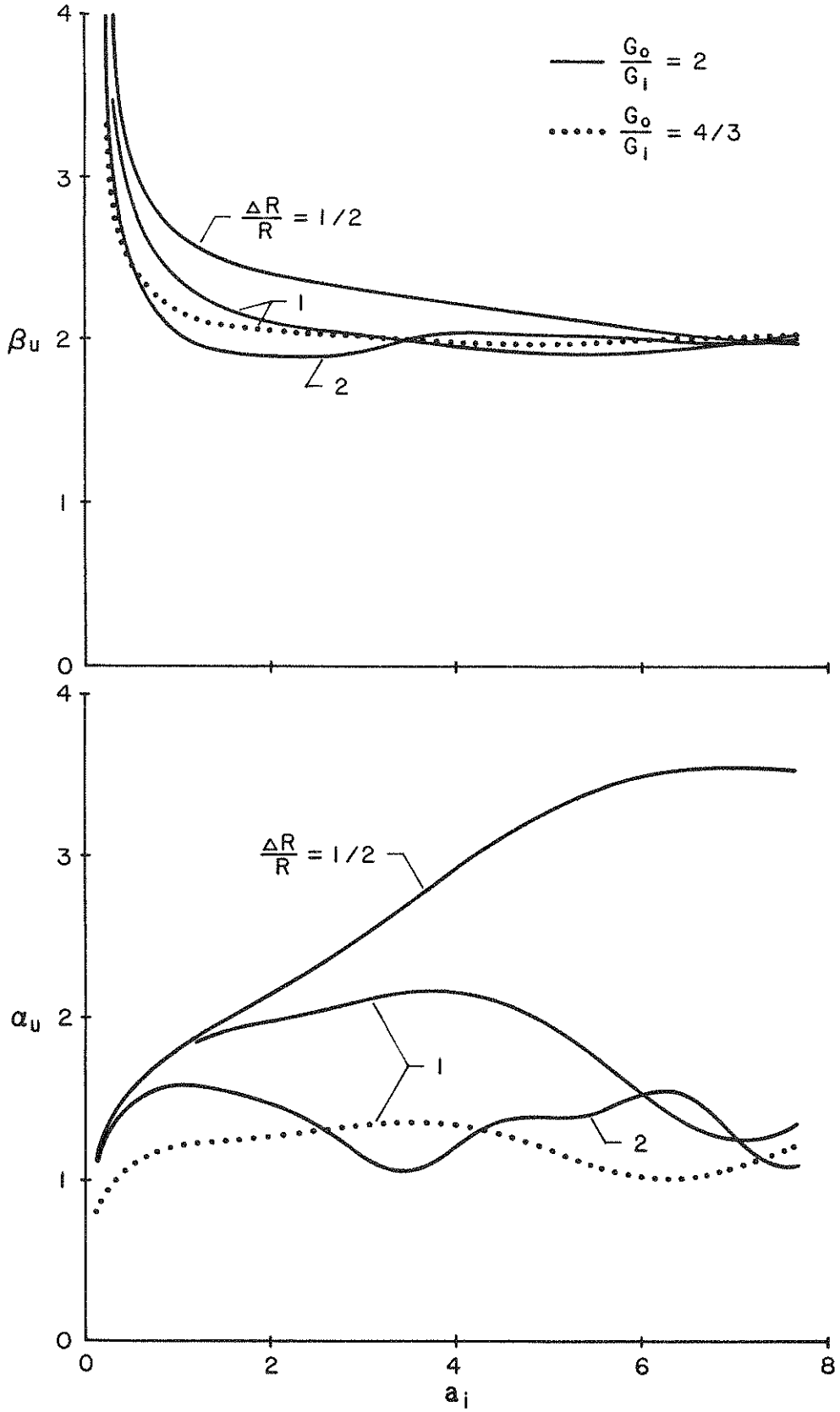

FIGURE 4-3 High-Frequency Behavior of Impedance Coefficients for Elastic Layer with Linearly Increasing Shear Modulus within Boundary Zone; $\nu = 1/3$

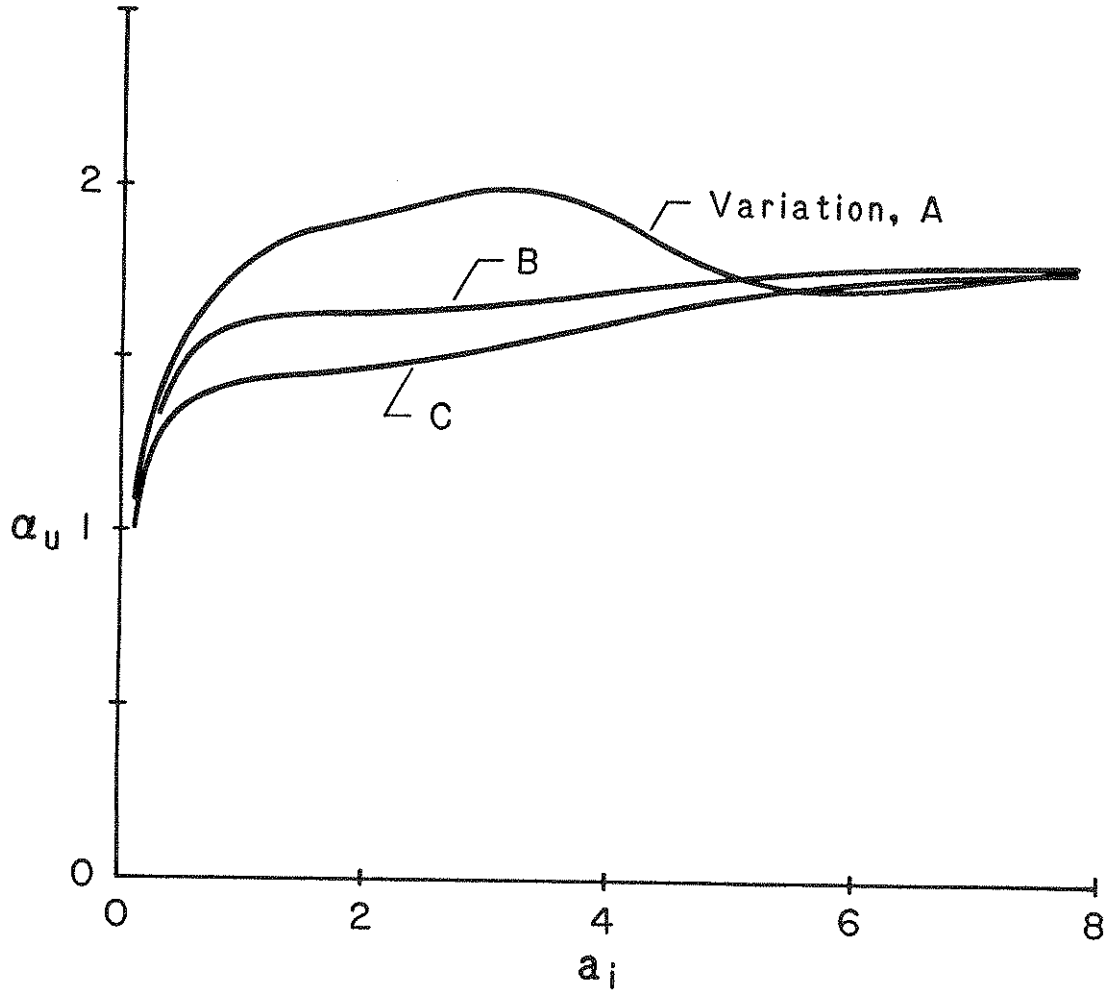

FIGURE 4-4 High-Frequency Behavior of Stiffness Coefficient for Elastic Layers with Variations in Shear Modulus Defined by Equation (26); $G_o/G_i = 2$; $f'(1) = 1$, $\nu = 1/3$

$$G(\xi) = G_i[1 + \sin(\xi - 1)] \qquad \text{for } 1 \leq \xi \leq 1 + \frac{\pi}{2}$$
$$= 2G_i = G_o \qquad \text{for } \xi \geq 1 + \frac{\pi}{2} \tag{26a}$$

variation 'B' is defined by

$$G(\xi) = G_i[2 - e^{-(\xi-1)}] \qquad \text{for } \xi \geq 1 \tag{26b}$$

and variation 'C' is defined by

$$G(\xi) = G_i\left[2 - \frac{1}{\xi}\right] \qquad \text{for } \xi \geq 1 \tag{26c}$$

Note that all three curves have the same high-frequency limit.

From solutions such as these and by analogy to the results for vertically and torsionally excited layers presented in Reference [11], the following approximate relation has been developed for the high-frequency limit of α_u when $\nu = 1/3$:

$$\alpha_u\big|_{a_i \to \infty} = 1 + 0.8\, f'(1) \tag{27}$$

in which $f'(1)$ = the value of G_i' normalized with respect to G_i. For the ramp-like linear variation of $G(\xi)$ emphasized in this paper, the function $f'(1)$ in equation (27) is given by

$$f'(1) = \left(\frac{G_o}{G_i} - 1\right)\frac{R}{\Delta R} \tag{28}$$

However, because $G'(\xi)$ is discontinuous at ξ_o, α_u has no well-defined high-frequency limit, and equation (27) in this case defines the horizontal asymptote about which the high-frequency values of α_u oscillate.

4.4 Effects of Nonlinear Variations in Material Properties

In Figure 4-5 are shown the impedance coefficients obtained for a layer with no material damping and a variation in $G(\xi)$ defined by

$$G(\xi) = G_i[-2(m+1) + 3(m+1)\xi - m\xi^2] \qquad \text{for } 1 \leq \xi \leq 2$$
$$= 4G_i = G_o \qquad \text{for } \xi \geq 2 \tag{29}$$

in which m is a constant. Three different values of m are considered: m =

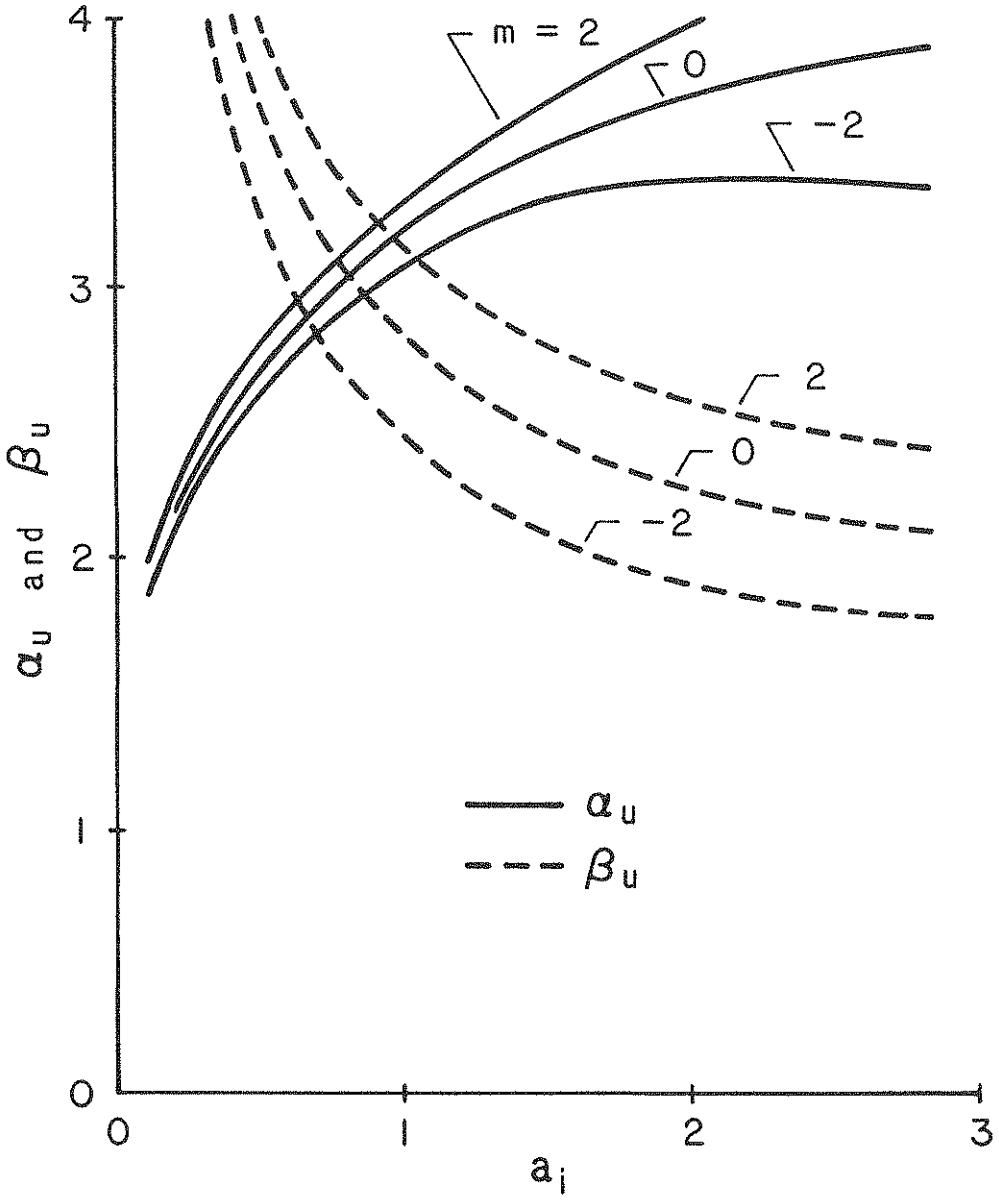

FIGURE 4-5 Impedance Coefficients for Elastic Layer with Variations in Shear Modulus Defined by Equation (29); $G_o/G_i = 4$, $\Delta R/R = 1$, $\nu = 1/3$

0, which corresponds to a linear variation; and m = 2 and m = -2, which correspond to variations that increase more rapidly and less rapidly, respectively, than the linear.

The general trends of the results displayed in Figure 4-5 could have been anticipated from the data presented in Figure 4-2. Since both α_u and β_u in Figure 4-2 generally increase with increasing G_o/G_i, an increase in the rate at which $G(\xi)$ approaches G_o would be expected to increase the values of the impedance factors, and a reduction in this rate would be expected to have the opposite effect.

As an indication of how the radial variation of material damping may affect the impedance factors, in Figure 4-6 are presented the values of α_u and β_u computed for a layer with $G_o/G_i = 4$ and $\Delta R/R = 1$ considering the three variations of $\tan\delta$ shown in the inset diagrams. Variation 'a' is defined by equation (25) and variations 'b' and 'c' are linear and constant, respectively. In all cases, the initial and terminal values of $\tan\delta$ are taken as 0.20 and 0.05, respectively, and the shear modulus within the boundary zone is considered to increase linearly.

Since G_i, G_i' and $\tan\delta_i$ for the data displayed in Figure 4-6 are the same, the three sets of curves behave similarly at the high values of the frequency parameter. However, the detailed variations of the curves at the lower frequencies are different, because the response of the layer in this range is affected by the properties of the layer over a fairly wide zone around the central hole, not merely by those at the inner boundary. Based on the data presented in Figure 4-1, the slower the radial decay of the material damping capacity of the layer, the higher would be expected to be the damping factor, β_u. By contrast, the effect on the stiffness factor, α_u, would be expected to be the opposite. These expectations are confirmed by the data presented in Figure 4-6.

4.5 Composite Layer with Constant Material Properties

In Figure 4-7 are shown the impedance coefficients for a composite layer of the type examined by Novak and Sheta [7], for which the shear modulus within each zone is assumed to be constant. The solid lines in this figure are for an elastic layer and the dashed lines are for a viscoelastic layer

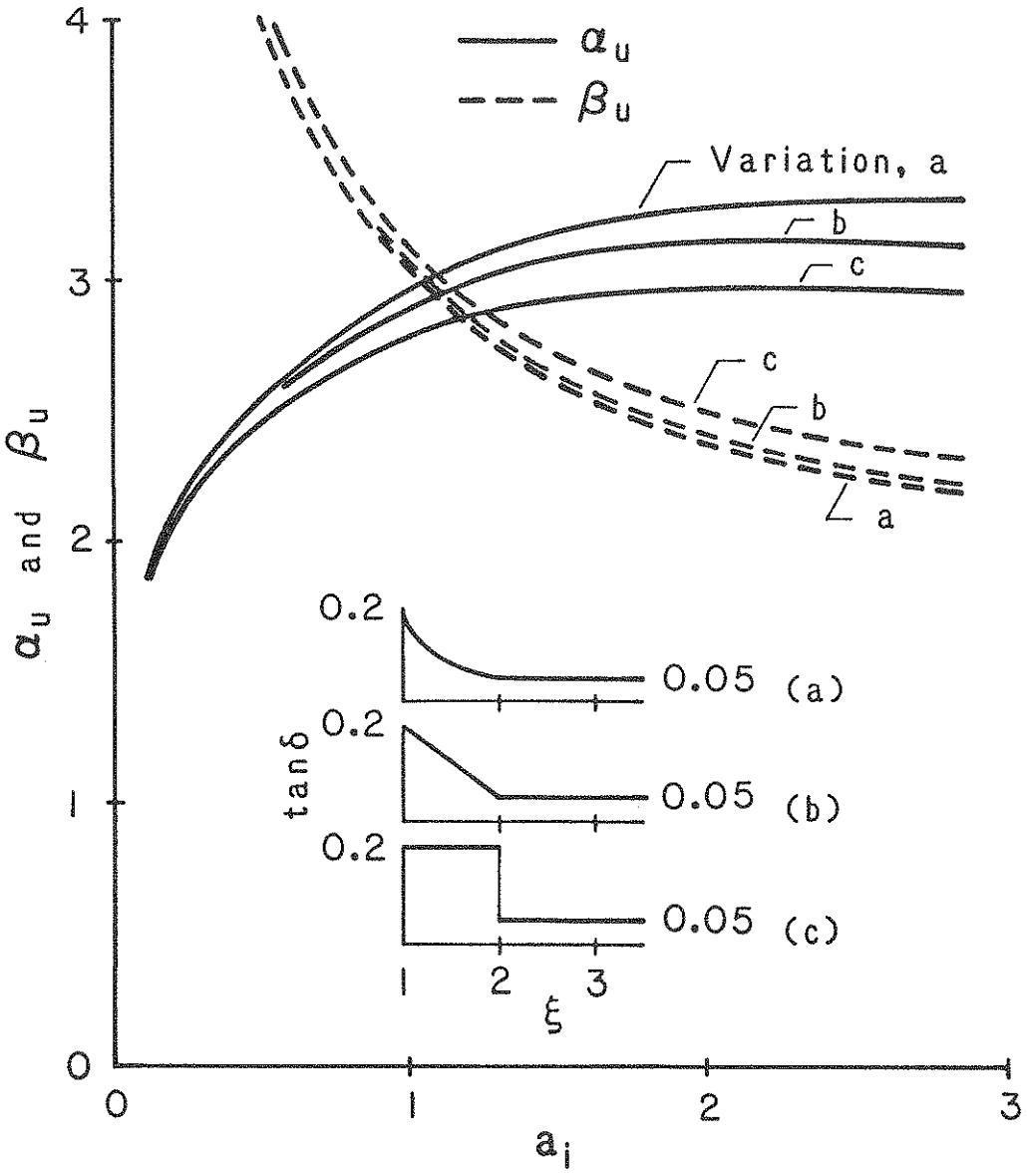

FIGURE 4-6 Impedance Coefficients for Viscoelastic Layer with Linearly Increasing Shear Modulus and Three Different Variations of Material Damping within Boundary Zone; $G_o/G_i = 4$, $\Delta R/R = 1$, $\nu = 1/3$

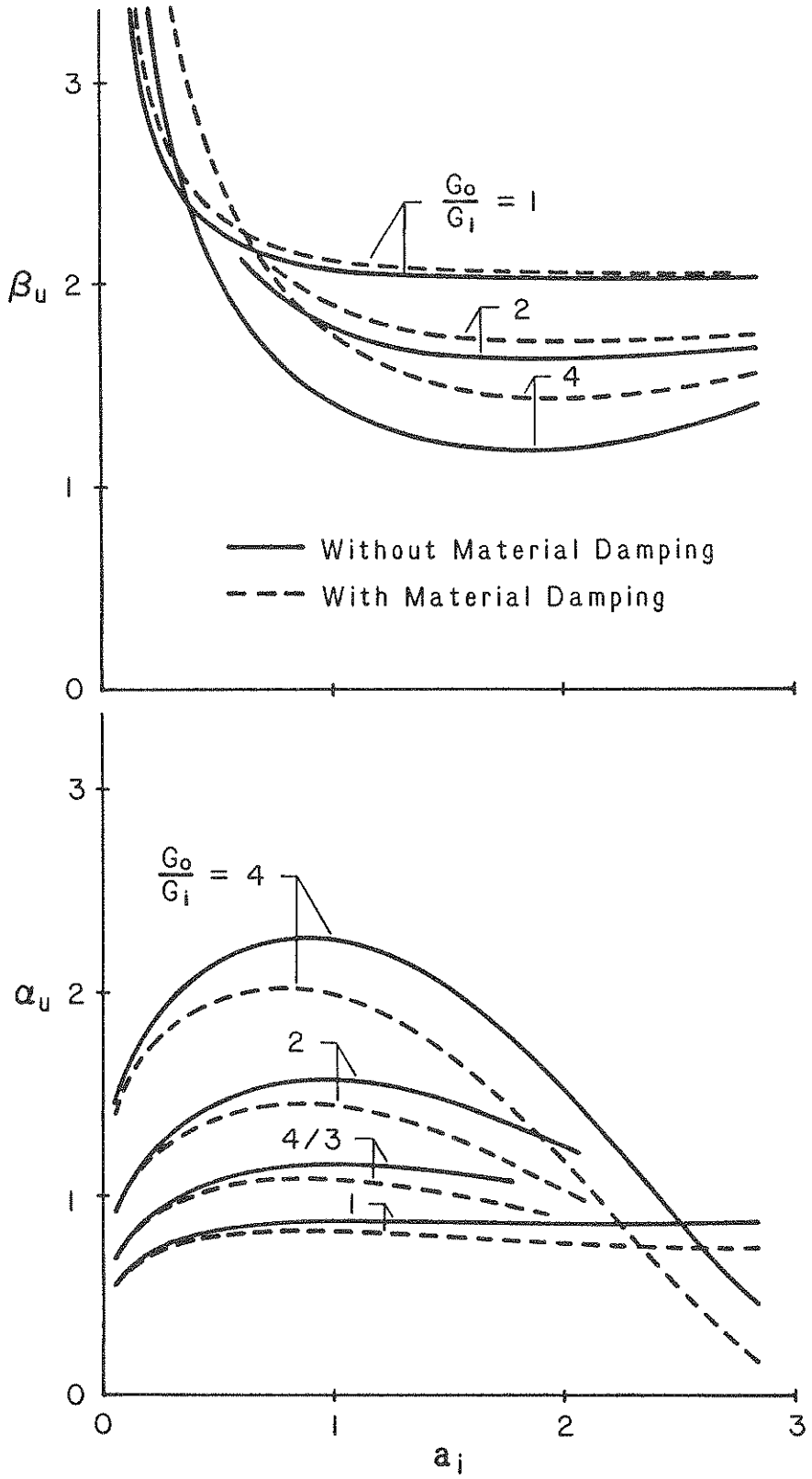

FIGURE 4-7 Impedance Coefficients for Layers with Constant Material Properties within each Zone; $\Delta R/R = 1$, $\nu = 1/3$

with $\tan\delta_i = (G_o/G_i)\tan\delta_o$ and $\tan\delta_o = 0.05$. The width of the boundary zone in these solutions is taken as $\Delta R/R = 1$. However, unlike the original Novak-Sheta solutions that were approximate, the present solutions are exact, and they were obtained by application of the method of analysis described herein taking $n = 1$.

It is instructive to compare the data in Figure 4-7 with those presented in part (d) of Figure 4-2 for layers with $\Delta R/R = 2$ and linearly increasing variations of shear modulus within the boundary zone. For the same values of G_o/G_i, the areas under the $G(\xi)$ diagrams in the two cases are the same. It is observed that the characteristics of the two sets of curves are similar, but that the amplitudes of the undulations for the curves in Figure 4-7 are substantially greater than for the curves in Figure 4-2(d). This indicates that the effects of wave reflections due to a discontinuity in $G'(\xi)$ are not nearly as important as those due to a discontinuity in $G(\xi)$.

It is also instructive to compare the solid curves in Figure 4-7 with the corresponding plots for vertically excited layers presented in Figure 2-3(d) of Reference [11]. Such comparison reveals that the two sets of data are similar except that the abscissa of the curves for the horizontally excited layer is a stretched version of that for the vertically excited layer. This difference stems from the fact that the fundamental natural frequency of the inner zone, p_1, is higher for the horizontal mode of vibration than for the vertical mode. The relative magnitudes of the two frequencies may be determined from Table 4-I, in which the values of the dimensionless coefficient c_1 in the expression

$$p_1 = c_1 \frac{v_{si}}{\Delta R} \tag{30}$$

are listed for several different values of $\Delta R/R$. Note that the natural frequency for the horizontal mode of vibration is approximately 50 percent greater than for the vertical mode. As a result, for the range of a_i values considered in Figure 4-7, the range of ω/p_1 values is effectively only two-thirds of that considered in the corresponding figure of Reference [11].

As a further consequence of this difference, within the practically important range of frequencies for which $a_i \leq 3$, the undulations of the curves

for layers with the abrupt variation in material properties are not as important for the horizontal mode of vibration as for the vertical. Accordingly, the simple step-like idealization of the shear modulus, which is clearly more convenient for purposes of analysis than the ramp-like variation, can be used with greater degree of confidence for laterally excited layers than for vertically excited layers.

TABLE 4-I. Values of Coefficient c_1 in Expression for Fundamental Natural Frequency of Inner Zone of Layer When its Outer Boundary is Fixed; $\nu = 1/3$

$\frac{\Delta R}{R}$	Value of c_1		Ratio of Columns $\frac{(2)}{(3)}$
	Horizontal Vibration	Vertical Vibration	
(1)	(2)	(3)	(4)
Value → 0	2.31	$\pi/2$	1.47
0.1	2.37	1.60	1.48
0.25	2.46	1.64	1.50
0.5	2.60	1.70	1.53
1.0	2.79	1.79	1.56
2.0	3.01	1.92	1.57

4.6 Comparison with Novak-Sheta Solution

The original Novak-Sheta (N-S) solution for a horizontally excited layer with a stepwise variation of shear modulus involves two fundamental assumptions: (1) That the inner zone is massless; and (2) that the circular boundary of the two zones remains circular during deformation.

As an indication of the errors that may result from these approximations, in Figure 4-8 are presented the impedance factors computed for a layer with $\Delta R/R = 0.5$, $G_o/G_i = 2$ and $\tan\delta = 0$. The long dashed lines in these plots represent the original N-S solution; the short dashed lines represent the solution obtained considering the inner zone to be massless but making no a priori assumption regarding the deformation of the interface of the two zones; and the solid lines represent the exact solution. Note that the errors resulting from the N-S approximations, particularly those stemming from the neglect of the mass of the inner zone, are indeed significant,

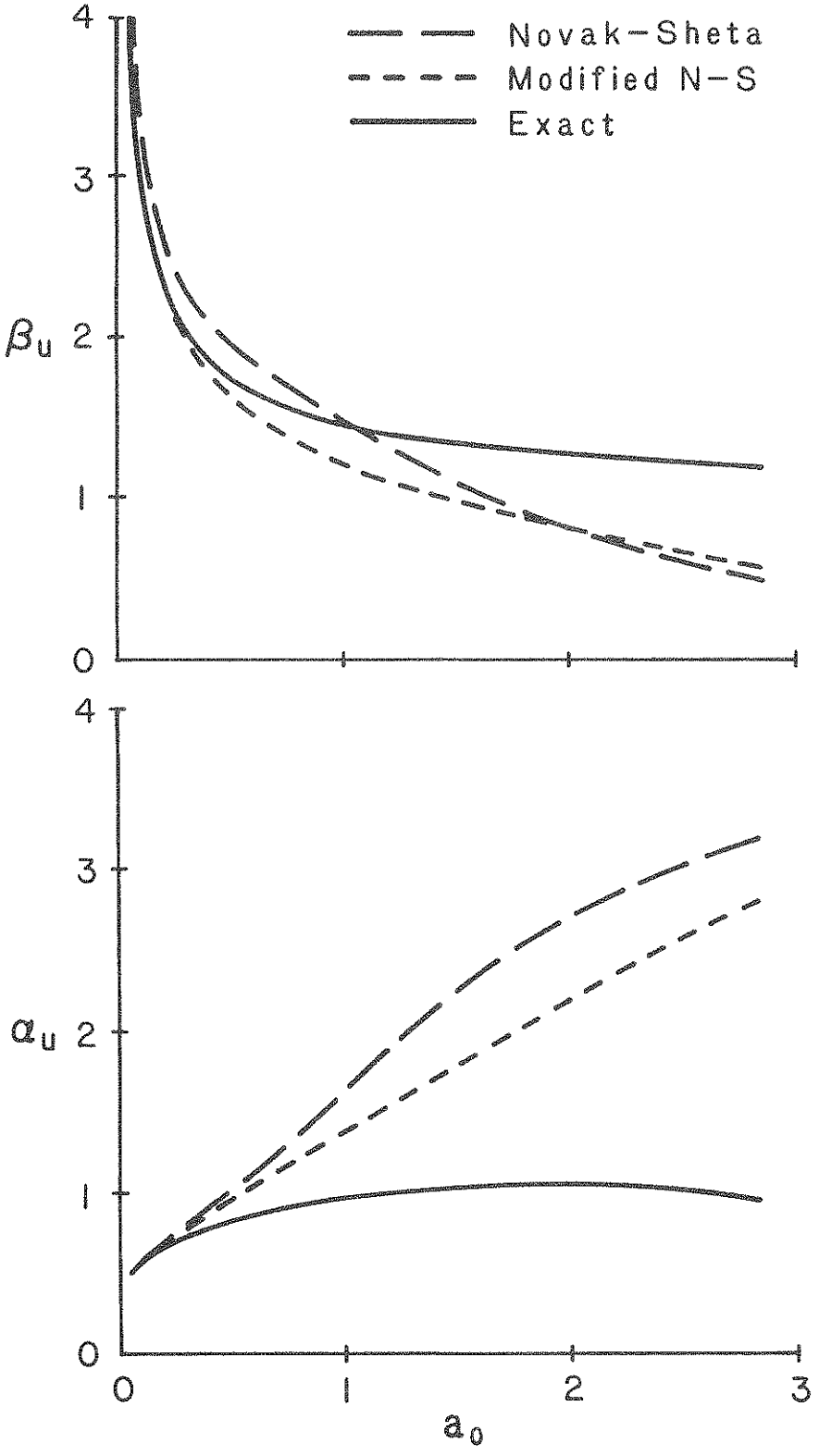

FIGURE 4-8 Effects of Novak-Sheta Idealizations on Impedance Coefficients for an Elastic Layer with Constant Material Properties within each Zone; $G_o/G_i = 2$, $\Delta R/R = 1/2$, $\nu = 1/3$

especially for the stiffness coefficients, α_u.

Within the range of frequencies considered, neglecting the mass of the inner zone effectively increases the stiffness of the layer and hence the values of α_u, and decreases its radiational energy dissipating capacity and hence the values of β_u. Similarly, considering the interface of the two zones to remain circular during deformation effectively constrains the soil layer and further increases its values of α_u.

The accuracy of the N-S solution would naturally be expected to be a function of the relative width of the boundary zone, $\Delta R/R$. The effect of this factor is demonstrated in Figure 4-9, in which the exact impedance coefficients for a homogeneous layer with no material damping are compared with those obtained by the original and modified versions of the N-S approach. The shear modulus for a fictitious boundary zone in the latter procedures is considered to be the same as for the remainder of the layer, and several different widths are used for the boundary zone. As would be expected, the differences between the exact and approximate solutions decrease with decreasing $\Delta R/R$, but the discrepancies are significant even for what might at first thought appear as relatively narrow boundary zones. The results of the proposed solution are, of course, identical to the exact results for all values of $\Delta R/R$. For a further explanation of these trends, reference may be made to Reference [10], in which similar comparisons have been made for vertically and torsionally excited layers.

4.7 Convergence and Accuracy of Solutions

The accuracy of the solution for a layer with radially varying shear modulus clearly depends on the number of ring elements employed in the solution. A measure of this accuracy is provided in Table 4-II, in which are listed the values of α_u and β_u obtained for an elastic layer with linearly increasing shear modulus within the boundary zone using a progressively larger number of elements of the same width. Several different combinations of G_o/G_i, $\Delta R/R$, and a_i are considered. It can be seen that the number of elements required for a solution of prescribed accuracy generally increases with increasing values of $\Delta R/R$, G_o/G_i and a_i, and that, in most cases, reasonable accuracy is achieved with as few as five elements.

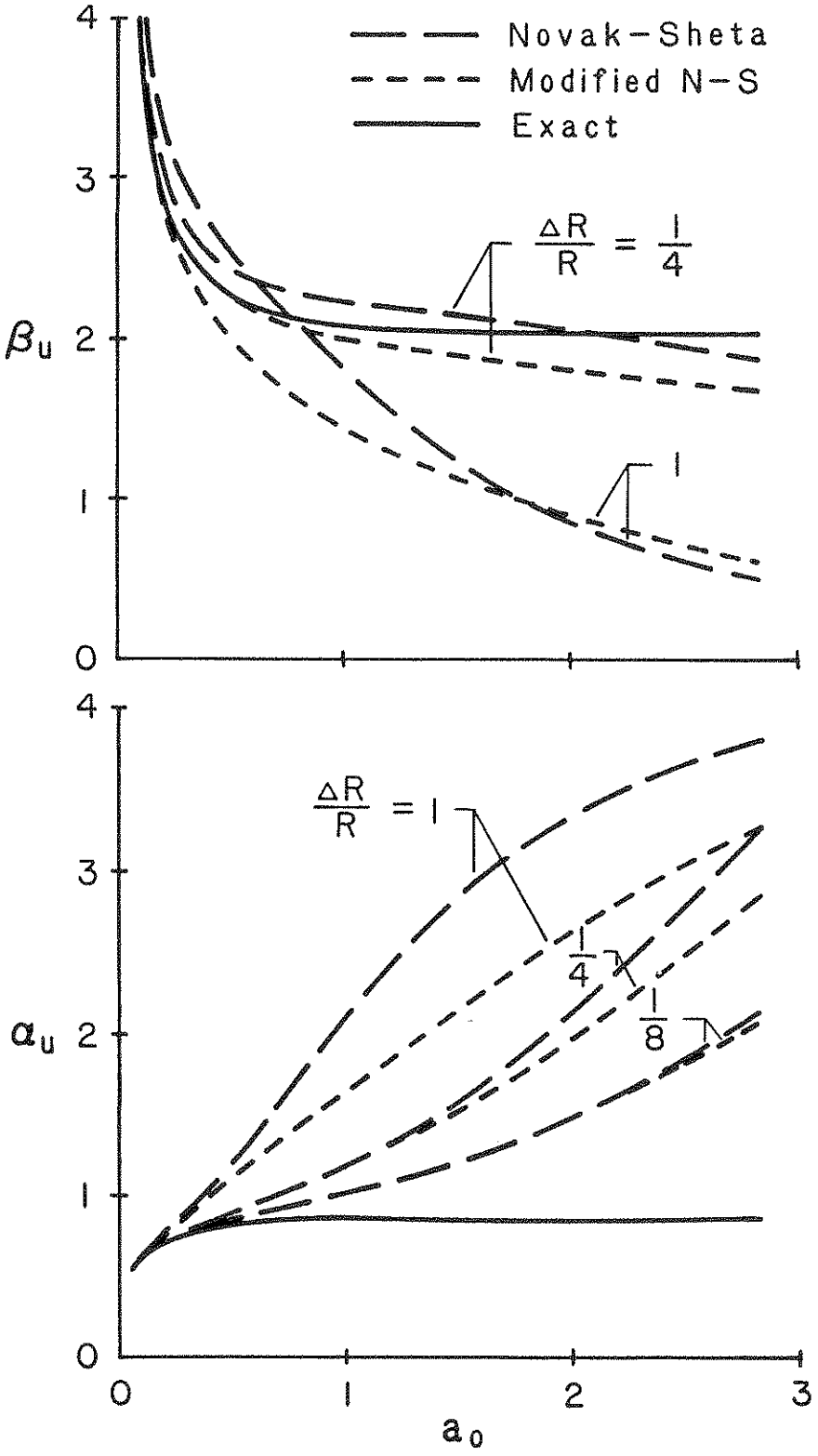

FIGURE 4-9 Effects of Novak-Sheta Idealizations on Impedance Coefficients for a Homogeneous Elastic Layer with $\nu = 1/3$

TABLE 4-II. Convergence of Impedance Coefficients for Elastic Layers with Linearly Increasing Shear Modulus Within the Boundary Zone; $\nu = 1/3$.

Number of Rings n	$G_o/G_i = 4/3$				$G_o/G_i = 4$			
	$a_i = 1$		$a_i = 3$		$a_i = 1$		$a_i = 3$	
	α_u	β_u	α_u	β_u	α_u	β_u	α_u	β_u
(1)	(2)	(3)	(4)	(5)	(6)	(7)	(8)	(9)
	(a) For $\Delta R/R = 1/4$							
1	1.22	2.27	1.60	2.11	3.33	2.98	4.91	2.07
5	1.19	2.34	1.49	2.21	3.41	3.75	5.05	3.05
10	1.19	2.34	1.47	2.23	3.40	3.85	4.93	3.19
20	1.19	2.35	1.46	2.23	3.40	3.90	4.87	3.25
30	1.19	2.35	1.45	2.23	3.40	3.91	4.85	3.27
50	1.19	2.35	1.45	2.24	3.40	3.92	4.83	3.29
	(b) For $\Delta R/R = 2$							
1	0.91	1.88	1.25	2.26	1.13	1.08	4.23	3.08
5	1.10	1.99	0.87	2.01	2.44	1.72	1.48	1.57
10	1.11	2.02	0.89	2.01	2.60	1.91	1.94	1.67
20	1.12	2.03	0.90	2.01	2.67	2.02	2.12	1.74
30	1.12	2.04	0.91	2.01	2.69	2.05	2.18	1.76
50	1.12	2.04	0.91	2.01	2.71	2.08	2.22	1.78

The solutions for the linear variation of shear modulus presented in this paper were obtained using from five to forty elements of the same width, giving due regard to the aforementioned trends. Somewhat larger numbers of elements were used for some of the other variations of $G(\xi)$ examined. The results presented are believed to be of high accuracy.

SECTION 5
PILE HEAD IMPEDANCES

This section demonstrates the influence that the radial inhomogeneity in soil properties may have on the dynamic impedances of piles subjected to horizontal or rotational motions at their heads. The piles are considered to be of solid circular cross section and hinged at the base, and their length-to-radius ratio is taken as $L/R = 40$. The soil properties are presumed to be independent of depth; the ratio of the mass densities for the pile and soil is taken as $\rho_p/\rho = 1.6$, a value that is representative of concrete piles; and the relative stiffness of the soil in contact with the pile and of the pile itself is expressed by the ratio $v_{si}/v_c = 0.025$, in which $v_c = \sqrt{E_p/\rho_p}$ = the compressional wave velocity in the pile, and E_p = the corresponding Young's modulus of elasticity. Poisson's ratio for the soil is taken as $\nu = 1/3$, and no material damping is assumed for either the pile or the soil.

Let K_{uu} be the lateral impedance of the pile head, defined as the complex-valued horizontal force which when applied at the pile head is necessary to induce a horizontal harmonic displacement of unit amplitude without rotation at that level; and let $K_{\phi\phi}$ be the rotational impedance, defined as the corresponding complex-valued moment necessary to induce a harmonic rotation of unit amplitude without displacement. Similarly, let $K_{u\phi}$ and $K_{\phi u}$ be the cross impedances, which represent the horizontal force and bending moment at the pile head associated with the unit rotation and unit horizontal displacement, respectively. Naturally, $K_{u\phi} = K_{\phi u}$. These impedances may conveniently be expressed in the form

$$K_{uu} = (K_{st})_{uu}[\alpha_{uu} + ia_i\beta_{uu}] \tag{31a}$$

$$K_{u\phi} = (K_{st})_{u\phi}[\alpha_{u\phi} + ia_i\beta_{u\phi}] \tag{31b}$$

$$K_{\phi\phi} = (K_{st})_{\phi\phi}[\alpha_{\phi\phi} + ia_i\beta_{\phi\phi}] \tag{31c}$$

in which $(K_{st})_{uu}$, $(K_{st})_{u\phi}$ and $(K_{st})_{\phi\phi}$ are the corresponding static stiffnesses of the pile when embedded in a homogeneous soil with properties equal to those of the soil in contact with the pile; and α_{uu} through $\beta_{\phi\phi}$

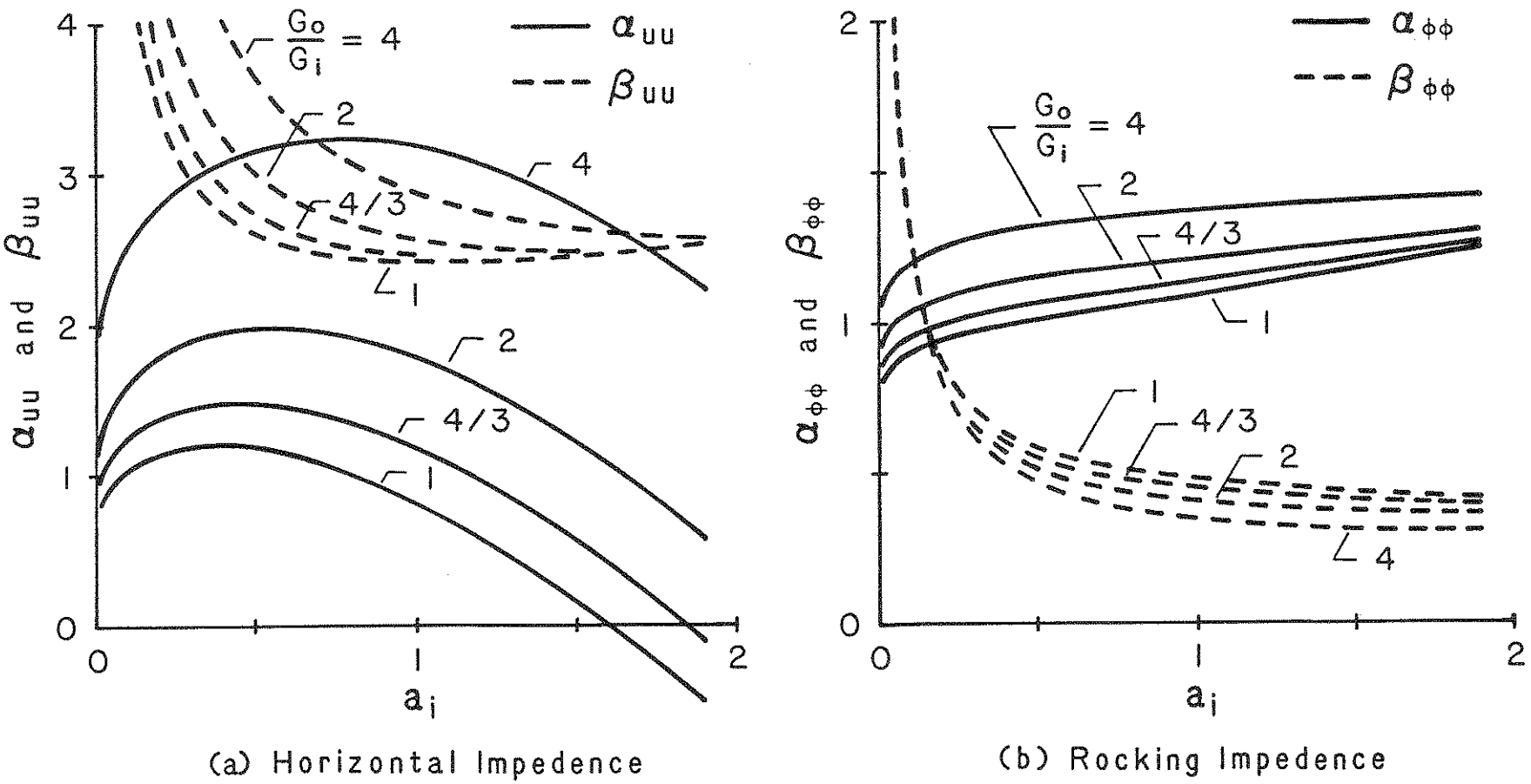

FIGURE 5-1 Impedance Coefficients for Hinged-Tip Piles in an Elastic Medium with Linearly Increasing Shear Modulus within Boundary Zone; for properties of piles and medium, see text (Figure continued)

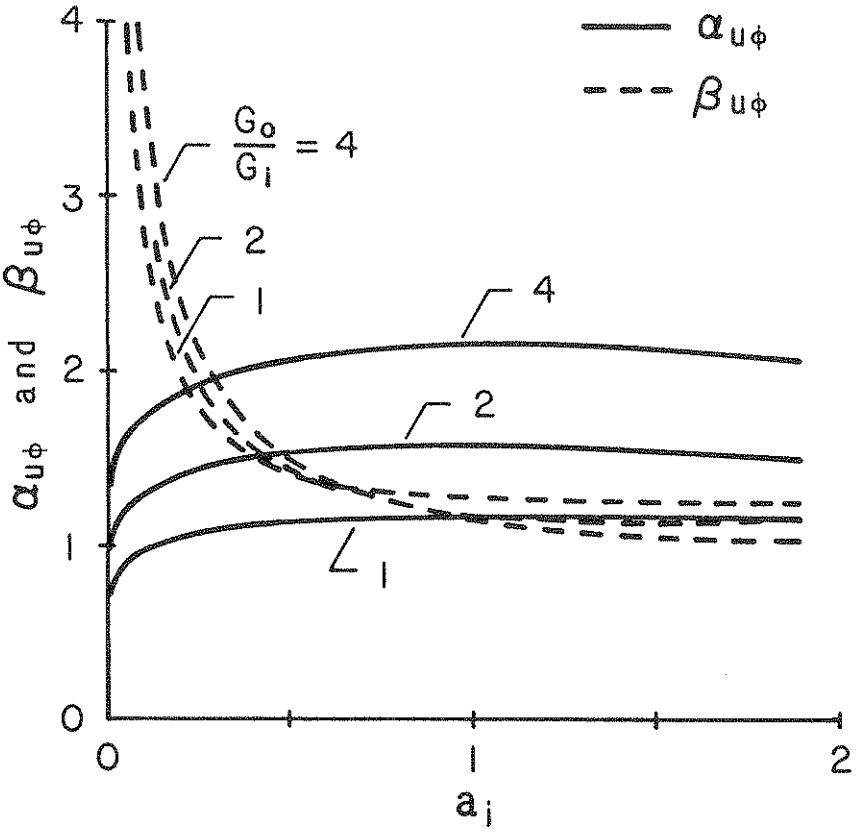

(c) Cross Impedences

FIGURE 5-1 Concluded

are dimensionless factors that depend on the relative properties of the soil and pile. The static stiffnesses were determined from Reference [8] to be $(K_{st})_{uu} = 20.60\, G_i R$, $(K_{st})_{u\phi} = 81.44\, G_i R^2$, and $(K_{st})_{\phi\phi} = 629.8\, G_i R^3$.

The factors α_{uu} through $\beta_{\phi\phi}$ were evaluated from the solutions of the differential equation of motion for the pile given in Reference [4], making use of the appropriate layer impedances presented in the preceding sections. In conformity with the approach used in Reference [4], the contribution of the rotatory resistance of the soil layers was not included in these solutions.

In Figure 5-1 are presented the results obtained for piles embedded in a composite medium for which the shear modulus within the boundary zone increases linearly in the horizontal or radial direction. The width of the boundary zone is taken as $\Delta R/R = 0.5$, and several different values of G_o/G_i are considered.

It is observed that the effects of horizontal inhomogeneity in soil properties may be quite substantial, and that the effects are greatest for the lateral impedance and least for the rotational impedance. It is further observed that the effects on α_{uu} and β_{uu} are very similar to those for the corresponding layer impedances (see the solid curves in Figure 4-2b).

Comparison of the data presented in Figure 5-1 with the corresponding data obtained for an infinitely long pile of the same cross sectional dimensions reveals that the two sets of results are for all practical purposes identical. The relevant impedances for infinitely long piles are given by the following simple expressions,

$$K_{uu} = 4\chi_p^3 \frac{E_p I_p}{R^3} \tag{32a}$$

$$K_{u\phi} = K_{\phi u} = 2\chi_p^2 \frac{E_p I_p}{R^2} \tag{32b}$$

$$K_{\phi\phi} = 2\chi_p \frac{E_p I_p}{R} \tag{32c}$$

in which I_p = the moment of inertia of the pile cross section about a horizontal centroidal axis, and

$$\chi_p = \sqrt[4]{\frac{G_i}{E_p}\left[1.5(\alpha_u + ia_i\beta_u) - a_i^2\frac{\rho_p}{\rho}\right]} \tag{33}$$

These expressions, in somewhat different form, appear to have been first presented in Reference [9].

SECTION 6
CONCLUSION

With the information and the method of analysis that have been presented, the dynamic impedances of horizontally excited, radially inhomogeneous viscoelastic soil layers with a circular hole, and the horizontal and rotational impedances of piles in a medium represented by such layers may be evaluated readily. The numerical data and the explanations that have been presented provide valuable insight into the effects and relative importance of the numerous factors involved.

SECTION 7
NOTATION

a_i	dimensionless frequency parameter for inhomogeneous layer, defined by equation (17)
a_o	dimensionless frequency parameter for homogeneous layer
A_j	constant of integration for jth ring
B_j	constant of integration for jth ring
c_1	coefficient in expression for p_1
C_j	constant of integration for jth ring
$[d_j(\xi)]$	matrix of order 4 x 4 that relates $\{S_j(\xi)\}$ to $\{X_j\}$
$[d_o(\xi)]$	matrix of order 4 x 2 that relates $\{S_o(\xi)\}$ to $\{X_o\}$
$[\tilde{d}_1(1)]$	matrix of order 2 x 4 the elements of which are identical to those of the first two rows of $[d_1(1)]$
D_j	constant of integration for jth ring
E_p	Young's modulus of elasticity for pile
$f'(1)$	slope of $G(\xi)$ at $\xi = 1$ normalized with respect to G_i
$G(\xi)$	shear modulus of elasticity for material of layer at ξ
G_i	shear modulus of elasticity for material of layer at the edge of the hole
G_i'	first derivative of $G(\xi)$ at boundary of central hole
G_j	shear modulus of elasticity for material of jth ring
G_o	shear modulus of elasticity for material of layer in undisturbed outer zone
G^*	complex-valued shear modulus of elasticity
i	$\sqrt{-1}$
I_p	moment of inertia of the pile cross section about a horizontal centroidal axis
I_κ	modified Bessel function of first kind of order κ

K_κ	modified Bessel function of second kind of order κ
$(K_{st})_{uu}$	static lateral stiffness of pile head
$(K_{st})_{u\phi}$	static cross stiffness (lateral force for unit rotation) of pile head
$(K_{st})_{\phi\phi}$	static rotational stiffness of pile head
K_u	dynamic horizontal impedance of soil layer
K_{uu}	dynamic lateral impedance of pile head
$K_{u\phi}$	dynamic cross impedance (lateral force for unit rotation) of pile head
$K_{\phi\phi}$	dynamic rotational impedance of pile head
m	constant in equation (29) that defines variation of $G(\xi)$
n	number of substitute rings
p_1	fundamental circular natural frequency for inner zone of layer when its outer boundary is fixed
r	radial distance to arbitrary point
r_j	radius of inner boundary of jth ring
R	radius of central circular hole and of pile
R_o	radius of interface of inner and outer zones of soil layer
$\{S_j(\xi)\}$	vector of displacement and stress amplitudes for jth ring
$\{S_o(\xi)\}$	vector of displacement and stress amplitudes for outer zone
t	time
$\tan\delta$	material damping factor when $\tan\delta_\ell$ and $\tan\delta_s$ are the same
$\tan\delta_i$	value of $\tan\delta$ for material at boundary of the central hole
$\tan\delta_\ell$	material damping factor for longitudinal distortion
$\tan\delta_o$	value of $\tan\delta$ for undisturbed outer zone
$\tan\delta_s$	material damping factor for shearing distortion
[T]	4 x 2 transfer matrix relating $\{X_1\}$ and $\{X_o\}$
u	radial component of displacement for arbitrary point on layer

U_j	complex-valued amplitude of radial displacement component for jth ring
v	circumferential component of displacement for arbitrary point on layer
v_c	longitudinal or compressional wave velocity in pile
v_ℓ	longitudinal wave velocity for material in a homogeneous layer
v_s	shear wave velocity for material in a homogeneous layer
v_{si}	shear wave velocity for material at the boundary of the central hole
v_{sj}	shear wave velocity for material of jth substitute ring
V_j	complex-valued amplitude of circumferential displacement component for jth ring
$\{X_j\}$	vector of constants of integration for jth ring
$\{X_o\}$	vector of constants of integration for the outer zone
$\{X_1\}$	vector of constants of integration for the ring adjoining the central hole
α_u	stiffness coefficient for soil layer
α_{uu}	stiffness coefficient for lateral impedance of pile head
$\alpha_{u\phi}$	stiffness coefficient for cross impedance of pile head
$\alpha_{\phi\phi}$	stiffness coefficient for rotational impedance of pile head
β_u	damping coefficient for soil layer
β_{uu}	damping coefficient for lateral impedance of pile head
$\beta_{u\phi}$	damping coefficient for cross impedance of pile head
$\beta_{\phi\phi}$	damping coefficient for rotational impedance of pile head
ΔR	width of disturbed boundary zone
ε	ratio of longitudinal and shear wave velocities for material of layer
θ	angle measured counterclockwise from an axis parallel to the direction of the applied force

λ	dimensionless parameter defined by equation (10a)
λ_j	value of λ for the jth ring
Λ	second Lame constant
Λ^*	complex-valued second Lame constant
μ	dimensionless parameter defined by equation (10b)
μ_j	value of μ for the jth ring
ν	Poisson's ratio for material of layer
ξ	r/R = dimensionless radial position coordinate
ξ_{j+1}	r_{j+1}/R
ξ_o	R_o/R
ρ	mass density for material of layer
ρ_i	mass density for material at boundary of central hole
ρ_p	mass density of pile
σ_j	complex-valued amplitude of radial stress for jth ring
σ_r	radial stress at arbitrary point on layer
τ_j	complex-valued amplitude of shearing stress for jth ring
$\tau_{r\theta}$	shearing stress at arbitrary point on layer
ϕ	potential function
Φ	complex-valued amplitude of ϕ
χ_p	dimensionless parameter defined by equation (33)
ψ	potential function
Ψ	complex-valued amplitude of ψ
ω	circular frequency of excitation and of resulting steady-state response

SECTION 8

REFERENCES

1. Achenbach, J.D., "Wave Propagation in Elastic Solids," North-Holland Publishing Co., New York, New York, 1984, pp. 73-75.

2. Gazetas, G., and Dobry, R., "Simple Radiation Damping Model for Piles and Footings," *Journal of Engineering Mechanics*, ASCE, Vol. 110, No. 6, June 1984, pp. 937-956.

3. Lakshmanan, N., and Minai, R., "Dynamic Soil Reactions in Radially Non-Homogeneous Soil Media," *Bulletin of the Disaster Prevention Research Institute*, Kyoto University, Vol. 31, Part 2, No. 279, June 1981, pp. 79-114.

4. Novak, M., "Dynamic Stiffness and Damping of Piles," *Canadian Geotechnical Journal*, Vol. 11, No. 4, 1974, pp. 574-598.

5. Novak, M., Nogami, T., and Aboul-Ella, F., "Dynamic Soil Reactions for Plane Strain Case," *Journal of the Engineering Mechanics Division*, ASCE, Vol. 104, No. EM4, August 1978, pp. 953-959.

6. Novak, M., Nogami, T., and Aboul-Ella, F., "Dynamic Soil Reactions for Plane Strain Case," *Research Report, BLWT-1-77*, Faculty of Engineering Science, The University of Western Ontario, London, Ontario, Canada, June 1977, pp. 1-26.

7. Novak, M., and Sheta, M., "Approximate Approach to Contact Effects of Piles," *Special Technical Publication on Dynamic Response of Pile Foundations: Analytical Aspects*, ASCE, M.W. O'Neill and R. Dobry, eds., October 1980, pp. 53-79.

8. Poulos, H.G., and Davis, E.H., *Pile Foundation Analysis and Design*, John Wiley and Sons, Inc., New York, New York, 1980, pp. 199-201.

9. Sanchez-Salinero, I. (supervised by J.M. Roesset), "Static and Dynamic Stiffnesses of Single Piles," *Geotechnical Engineering Report GR82-31*, Geotechnical Engineering Center, Civil Engineering Department, University of Texas, Austin, Texas, pp. 83-86.

10. Veletsos, A.S., and Dotson, K.W., "Impedances of Soil Layer with Disturbed Boundary Zone," *Journal of Geotechnical Engineering*, ASCE, Vol. 112, No. 3, March 1986, pp. 363-368.

11. Veletsos, A.S., and Dotson, K.W., "Vertical and Torsional Vibration of Foundations in Inhomogeneous Media," *Technical Report NCEER-87-0010*, National Center for Earthquake Engineering Research, State University of New York at Buffalo, June 1987.

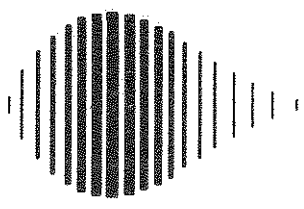

National Center for Earthquake Engineering Research
State University of New York at Buffalo